Thermochimica Acta, 154 (1989) 129–143
Elsevier Science Publishers B.V., Amsterdam – Printed in The Netherlands

CALORIMETRY OF HETEROGENEOUS SYSTEMS: H^+ BINDING TO TiO_2 IN NaCl *

SCOTT R. MEHR, DELBERT J. EATOUGH, LEE D. HANSEN, and EDWIN A. LEWIS **

Brigham Young University, Provo, UT 84602 (U.S.A.)

JAMES A. DAVIS

U.S. Geological Survey, Water Resources Div., Menlo Park, CA 94025 (U.S.A.)

(Received 13 February 1989)

ABSTRACT

A simultaneous calorimetric and potentiometric technique has been developed for measuring the thermodynamics of proton binding to mineral oxides in the presence of a supporting electrolyte. Modifications made to a commercial titration calorimeter to add a combination pH electrode and maintain an inert atmosphere in the calorimeter reaction vessel are described. A procedure to calibrate potentiometric measurements in heterogeneous systems to correct for the suspension effect on pH is given.

The enthalpy change for proton dissociation from TiO_2 in aqueous suspension as a function of pH is reported for 0.01, 0.1, and 0.5 M NaCl. The enthalpy change for proton dissociation is endothermic, ranging from 10.5 ± 3.8 to 45.0 ± 3.8 kJ mol^{-1} over the pH range from 4 to 10.

INTRODUCTION

A detailed thermodynamic description of reactions at the solid–solution interface of mineral oxides would be useful in furthering our understanding of processes such as ore deposition, metal extraction, weathering, and in modeling the transportation of trace contaminants in ground water. Gibbs free energy, ΔG°, data on ion interactions with the surface of mineral oxides are abundant [1–15], and many surface complexation models have been proposed. However, knowledge of the distribution of ions bound at the solid–solution interface and a theoretical basis for understanding the thermodynamics of ion binding are lacking [16]. Westall and Hohl [17] reviewed

* Dedicated to Professor James J. Christensen in memory of his contribution to innovation in calorimetry.

** Author to whom correspondence should be addressed.

0040-6031/89/$03.50

five surface complexation models and concluded that all five fit the potentiometric data at one ionic strength equally well. They further state that none of the models yield an unambiguous theoretical description of the relative importance and magnitude of electrostatic and chemical contributions to adsorption energies for binding at the mineral oxide surface. Separating ΔG into ΔH and ΔS contributions would be helpful in gaining more insight into the physicochemical processes involved in H^+ binding at the mineral oxide surface.

Others have reported free energy changes as a function of temperature and calculated ΔH for H^+ binding [8,18,19]. However, the required assumption that ΔH be constant with temperature may not hold because ΔC_p may be largely due to solvent/interface/surface reorganization. Determination of ΔH by calorimetry involves no assumptions; however, very little calorimetric data on ion binding to mineral oxides have been reported [20–22]. This paper describes a commercially available titration calorimeter specifically modified for the simultaneous determination of ΔG and ΔH for H^+ binding to mineral oxides in aqueous electrolyte solutions.

The study of suspensions by calorimetry presents a number of unique problems. For example, care must be taken to insure that the particles are dispersed and that particle concentration gradients, due to gravity, are not significant. It must also be determined whether better potentiometric data can be obtained by simultaneous measurement with a pH electrode placed inside the calorimeter, or by measuring the pH in parallel experiments. Errors in hydrogen ion activity measurements resulting from suspensions of charged particles must be minimized. The possible presence of slow kinetic effects due to surface reactions must be determined, e.g. Berube and de Bruyn [8] observed that pH shifts may be seen for months as ions are absorbed or released from rutile after an aliquot of titrant is added.

EXPERIMENTAL

All solutions and suspensions were prepared with freshly boiled, deionized–distilled water and stored in polyethylene containers. Basic solutions were stored in polyethylene containers fitted with carbon dioxide absorbent cartridges, Mallinckrodt Mallcosorb, to prevent CO_2 adsorption. TiO_2-P25, purchased from Degussa Inc., Petersburo, NJ, was used in this study. This TiO_2, 60% anatase and 40% rutile, was acid washed, copiously rinsed with deionized water, and freeze dried for storage. The primary particles have a median size of 20 nm with a range of 10–30 nm. The surface area is 47 $m^2\ g^{-1}$ by N_2 BET and the point of zero charge, PZC, is at pH 6.4 in NaCl solution. Fresh stock suspensions, 5% by weight of TiO_2, were prepared frequently throughout the study in order to keep conditions as uniform and consistent as possible. In a neutral solution the particles tend to

coagulate, so the pH of the stock suspension was adjusted to less than 3 with HCl in order to minimize particle aggregation and CO_2 contamination. Approximately 100 ml of the stock suspension in a brown glass bottle was placed in a 2.5 l, 120 watt ultrasonic bath filled with water and sonicated for 24 hours, then stirred for another three days prior to use. The stock suspension was kept at room temperature (21° C) and continuously stirred until discarded. A new stock suspension was prepared at least every two months.

A Tronac Model 450 titration calorimeter equipped with two, constant rate, 2.5 ml, burets (0.106 ml min^{-1}) was used in this study. The calorimetric data were digitized with a Keithley model 195A digital volt meter and saved on a Commodore C64 computer. The pH header available for the Tronac calorimeter employs a saturated KCl,Ag/AgCl electrode with a high reference electrolyte flow rate. To study ionic strength effects, during long experiments, a very slow flow rate of reference electrolyte must be used. So the usual micro electrode used with the Tronac calorimeter was replaced with a gel-filled Orion, 91-15, micro-combination electrode. A Corning, model 150 pH/ion meter, was used to measure the pH. The analog output from the pH meter was digitized with another Keithley model 195A DVM and the data were saved with the C64 computer along with the calorimetric data. All the data were transferred to a Vax 8600 computer for analysis.

The suspensions to be titrated were prepared by adding 6 ml of the 5% stock suspension into 24 ml of 0.01, 0.1, or 0.5 M NaCl, and placing the diluted suspension in the ultrasonic bath for 15 minutes while bubbling argon through the suspension. After sonication, 25 ml of the suspension was pipetted into the calorimeter reaction vessel, the calorimeter was purged with Ar, the pH was adjusted to approximately 4 with HCl, and the temperature was adjusted to 25.0° C with the calibration heater. The titration cycle consisted of a 7 min lead period, followed by titration with base to about pH 10 (1 ml of 0.1 M NaOH) requiring 10 min, a 14 min trail/lead period, a titration to pH 4 with acid (1 ml of 0.1 M HCl, 10 min), a 7 min trail period, and a repeat of the entire cycle with the same sample. Experiments were done in triplicate. In addition, blank titrations were done with the same procedure, except that no TiO_2 was added. The C64 computer was used to control operation of the burets during an experiment.

The calorimetric data were corrected for non-chemical heat effects using previously published procedures [23]. Slight variations in the starting pH for replicate titrations were accounted for by referencing the heat (Q) data and the equivalents (n) of titrant added from the PZC. The amount of surface reaction was calculated by subtracting the number of equivalents of titrant required to titrate the blank from the number of equivalents required to titrate the suspension over the identical pH range. Similarly, the heat associated with the surface reaction was calculated by subtracting the heat of titration of the blank from the heat of titration of the suspension over

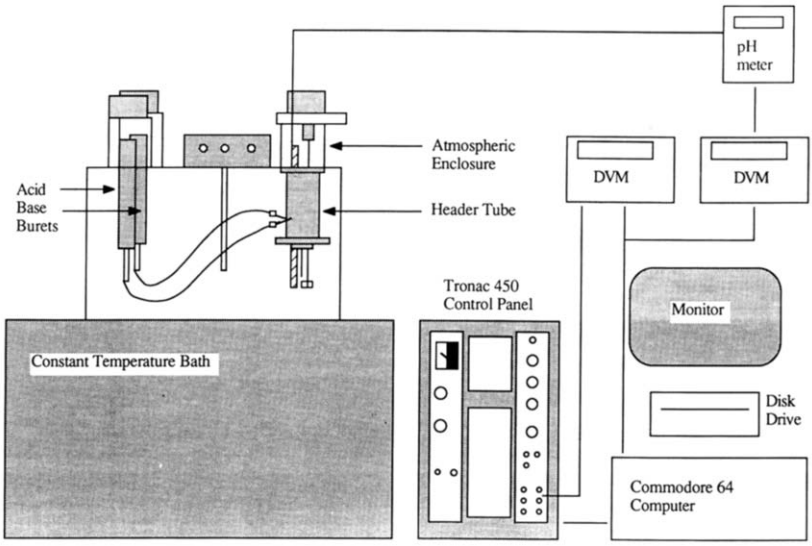

Fig. 1. Block diagram of the calorimetric system showing the modified header tube large enough to include an Orion micro combination pH electrode and showing the attached atmospheric enclosure.

identical pH range. Corrections for the heat of titrant dilution were ignored as the worst case for the heat of dilution of the titrant was found to be negligible, i.e. much less than the noise in the data.

Experiments to determine the optimum stirring configuration were performed with silica sand in a transparent dummy reaction vessel. Silica (0.25–0.5 g, 30–40 mesh) was placed in the reaction vessel and the particle distribution observed at various stirring speeds for both clockwise and counter-clockwise rotations. A 1.5 cm, two-blade propeller with a left hand twist (so that clockwise rotation lifted the particles up the stirring rod shaft with the particles falling back down along the sides of the reaction vessel) was used. Appropriate stirring was obtained with a clockwise, 1000 Rev min^{-1} motor.

The pH of a suspension exposed to air over several hours will drift because of CO_2 absorption. Therefore a sealed, Plexiglas enclosure was added between the stirring motor and the header tube of the calorimeter (see Fig. 1) so that CO_2 could be excluded from the reaction vessel. Before titrating a sample, the reaction vessel, header tube, and atmosphere enclosure were purged with argon.

To obtain accurate reference potentials in suspensions of charged particles, an adequate outward flux of reference electrolyte through the junction surface must be provided by either diffusion or flow. But such an electrode could not be used in this study because the reference electrolyte would alter the ionic strength. A non-flowing gel-type reference electrode with thick junctions gives readings that are erroneous [24], but that are reproducible.

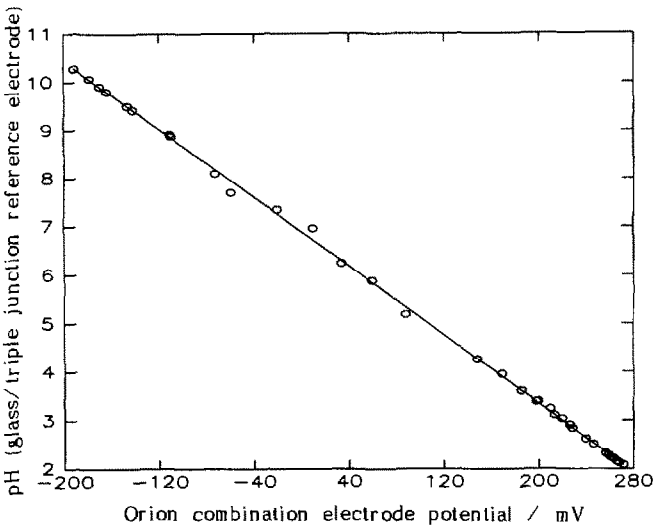

Fig. 2. A plot of the pH electrode calibration data. The points shown are for the pH measured with a Fisher 13-620-284 glass electrode and an Ag/AgCl triple junction reference electrode plotted versus the potential measured with an Orion 91-15 micro-combination pH electrode. The Orion pH electrode was the same pH electrode used in the calorimetric experiments. The calibration data shown are for an experiment where both electrode systems were placed in the same TiO_2 suspension (10 g l^{-1} in 0.1 M NaCl) at 25 °C. The solid line is a linear least-squares fit of the data with a slope of −0.0182 pH mV^{-1} and an intercept of 7.05 pH.

Therefore, the gel-filled electrode was calibrated against an electrode that had an adequate outward flow of reference electrolyte solution. The combination electrode in the calorimeter was calibrated against a Fisher, 13-620-284, glass electrode and Ag/AgCl triple-junction reference electrode in a TiO_2 suspension that was titrated with acid and base. The calibration electrode system was previously calibrated with two NBS standard reference pH buffers (NBS-SRM 189a, potassium tetroxalate, pH at 25 °C is 1.681, and NBS-SRM 186-I-c/186-II-c, potassium dihydrogen phosphate/disodium hydrogen phosphate, pH at 25 °C is 6.863). All calibrations were done at 25 °C (see Fig. 2).

A block diagram of the calorimeter system with the modifications noted is shown in Fig. 1. Detailed engineering drawings of the modified calorimeter parts are available upon request from the authors.

RESULTS AND DISCUSSION

The equilibria describing proton dissociation reactions at the TiO_2 surface are

$$S\text{–}OH_2^+ = S\text{–}OH + H^+ \quad (1)$$

$$S\text{–}OH = S\text{–}O^- + H^+ \quad (2)$$

In order to study the above proton dissociation reactions, both acid and base titrations were done in the calorimeter. The reactions actually taking place in the calorimeter during titration are base titration:

$$S\text{–}OH_2^+ + OH^- \rightarrow S\text{–}OH + H_2O \quad (3)$$

$$S\text{–}OH + OH^- \rightarrow S\text{–}O^- + H_2O \quad (4)$$

and acid titration:

$$S\text{–}O^- + H^+ \rightarrow S\text{–}OH \quad (5)$$

$$S\text{–}OH + H^+ \rightarrow S\text{–}OH_2^+ \quad (6)$$

where S represents the crystal surface.

The charge at a proton binding site can be either $+1$, 0, or -1 as indicated by reactions (1) and (2) above. The average charge per site can take on non-integral values between $+1$ and -1 depending on the pH. The surface charge, σ, in microcoulomb per square centimeter ($\mu C\ cm^{-2}$), is calculated using eqn. (7)

$$\sigma = \frac{nF}{ws} \quad (7)$$

where n is the number of microequivalents of protons reacting with the surface, F is Faraday's constant, w is the weight of TiO_2 in grams in the suspension, and s is the surface area in $cm^2\ g^{-1}$. A plot of σ versus pH for TiO_2 in three different concentrations of NaCl is given in Fig. 3. The curves in Fig. 3 are averages of acid and base titrations of TiO_2 done in the

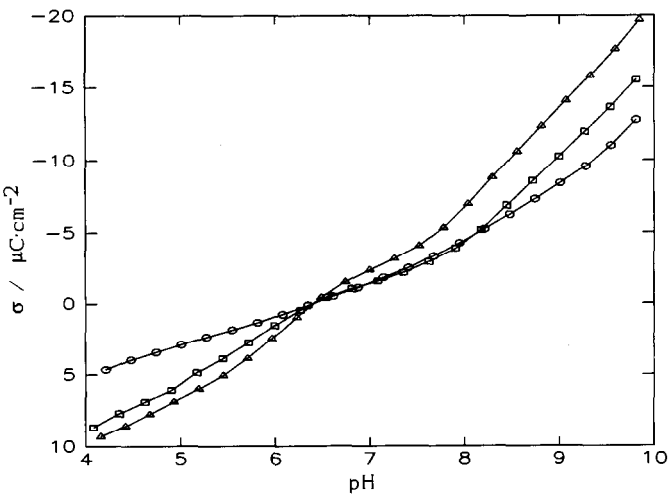

Fig. 3. A plot of σ (surface charge) in $\mu C\ cm^{-2}$ versus pH for TiO_2 in 0.01 M (○), 0.1 M (□), and 0.5 M (△) NaCl at 25 °C. The σ data were calculated from the potentiometric titration data collected simultaneously with the calorimetric data. The curves shown are averages of σ as observed in both the acid and base titrations.

calorimeter. The acid and base data were averaged in order to make a direct comparison with data in the literature. The averaged data obtained in combined calorimetric/potentiometric titration experiments are in agreement, with respect to shape and magnitude, with other TiO_2 surface charge curves [22,25–27]. Differences between our acid and base titrations or between our averaged data and data taken from the literature are attributable to the fact that our titrations were done more rapidly than any of the titrations previously reported. A plot of the acid and base surface charge curves, as calculated by averaging six acid titrations (with standard deviations ± 1.8 and ± 0.9 μC cm^{-2} for 0.01 and 0.5 M NaCl respectively) and by averaging six base titrations (standard deviations ± 2.1 and ± 1.0 μC cm^{-2} for 0.01 and 0.5 M NaCl respectively), are compared to the average surface charge curve, as calculated by averaging all of the twelve acid and base titrations together (with a standard deviation of ± 2.5 and ± 4.9 μC cm^{-2} for 0.01 and 0.5 M NaCl), for TiO_2 at two different ionic strengths in Fig. 4. The potentiometric data obtained in our experiments are sufficiently reproducible that the difference between the acid and base curves is significant. An explanation for this hysteresis is discussed later.

The enthalpy change for proton ionization was calculated by numerically differentiating the blank corrected heat versus equivalents data, i.e. $\Delta H_M = dQ/dn$, over a small pH interval (0.02–0.2 pH units) and is thus valid at the mean pH of the interval. Figure 5 shows ΔH_{H^+} versus pH for 0.5 M NaCl. All of the thermodynamic parameters reported are for proton ionization, i.e. reactions (1) and (2). In the case of the base titrations, ΔH_{H^+} for proton ionization is calculated from the overall ΔH_M measured for reactions (3) and (4) by eqn. (8).

$$\Delta H_{H^+} = \Delta H_M - \Delta H_{f,water} \tag{8}$$

In the case of the acid titrations, ΔH_{H^+} for proton ionization is calculated from the overall ΔH_M measured for reactions (5) and (6) by eqn. (9)

$$\Delta H_{H^+} = -\Delta H_M \tag{9}$$

ΔH_{H^+} as calculated in eqns. (8) and (9) includes the enthalpy change for proton ionization and counterion binding as shown in reactions (10) and (11)

$$S\text{–}OH_2^+ \cdot Cl^- \leftrightarrow S\text{–}OH + H^+ + Cl^- \tag{10}$$

$$S\text{–}OH + Na^+ \leftrightarrow S\text{–}O^- \cdot Na^+ + H^+ \tag{11}$$

In order to compare titrations done under different conditions, e.g. TiO_2 concentration, supporting electrolyte, or ionic strength differences, the titration data were fitted to eqn. (12)

$$\Delta H_{H^+} = A - B\frac{e^{[C(1/pH)-(1/D)]}}{1 + e^{[C(1/pH)-(1/D)]}} + E(pH - D) \tag{12}$$

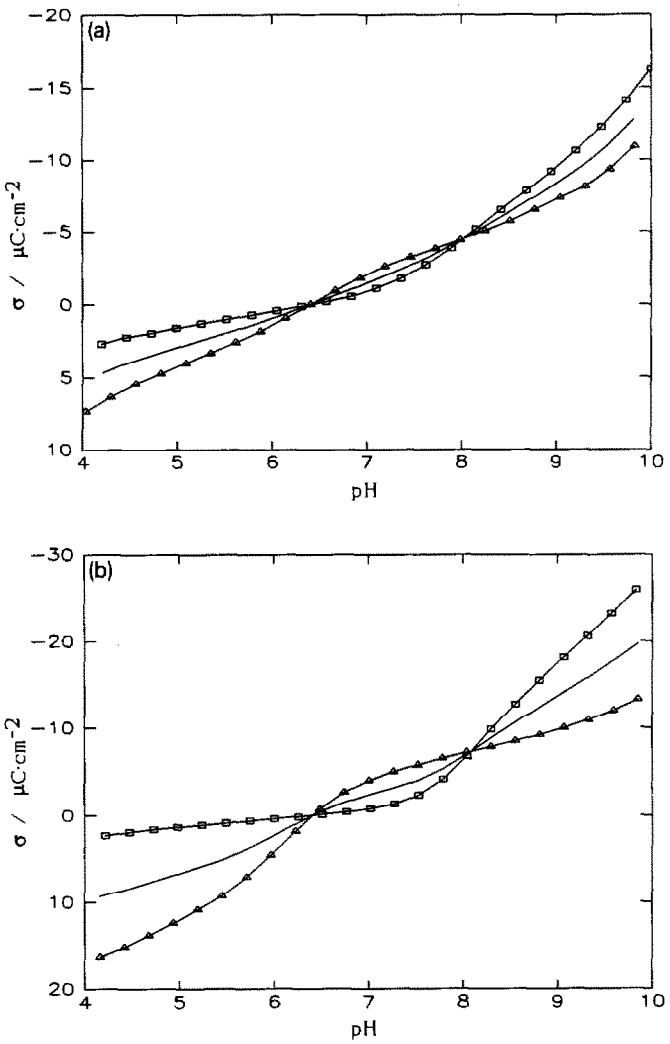

Fig. 4. Plots of σ (surface charge) in μC cm^{-2} versus pH for TiO_2 in 0.01 M (Fig. 4a) and 0.5 M (Fig. 4b) NaCl. The plots show the surface charge as calculated from the acid (□) and the base (△) titration data along with the average surface charge (———). Increasing ionic strength increases the hysteresis, i.e. the difference in the surface charge calculated at a given pH from the acid and base titration curves.

with five adjustable fitting parameters (A, B, C, D, and E). Equation (12) is an empirical formula that has the correct form to fit and smooth the titration curve, thus allowing different titration curves to be compared without distracting noise in the data for individual curves. The fitting parameters are possibly related to the following thermodynamic terms: A and B to ΔH_1 and ΔH_2, the intrinsic enthalpy changes for ionization of protons 1 and 2 where $A = \Delta H_2$ and $B = \Delta H_2 - \Delta H_1$; C to the fraction of positive and negative sites at a particular pH; D to pH^0, the pH at which

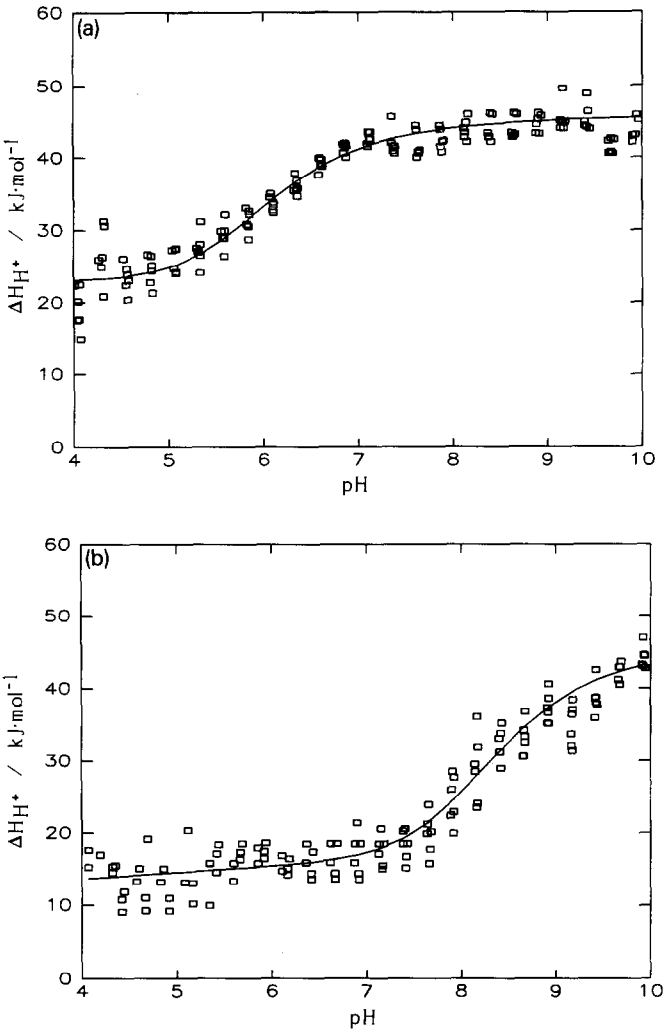

Fig. 5. ΔH_{H^+} in kJ mol^{-1} plotted versus pH for proton ionization from TiO_2 in 0.5 M NaCl. The points shown in Fig. 5a are the ΔH_{H^+} values calculated from six different base titration curves (two titrations on each of three different samples). The points shown in Fig. 5b are the ΔH_{H^+} values calculated from six different acid titration curves (two titrations on each of three different samples). The solid line shown, in both a and b, is the fit of the ΔH_{H^+} data with eqn. (12) and the fitting parameters given in Table 1.

the intrinsic ΔH values apply (ideally pH^0 would equal the PZC); and E to $\partial \Delta H/\partial pH$, the overall electrostatic enthalpy change with pH. Figure 5 shows both the data and the smooth fit for a typical TiO_2 titration. Equation (12) was found to fit all of the acid and base titration data equally well. The ΔH versus pH curves shown in subsequent figures were obtained by fitting the titration data using eqn. (12) with the corresponding fitting parameters given in Table 1.

Figure 6 shows both the acid and base titration data for ΔH_{H^+} versus pH for proton ionization from TiO_2 in 0.01, 0.1, and 0.5 M NaCl. The data obtained in this study are sufficiently reproducible that new features may be seen in the ΔH_{H^+} versus pH curves. It is clear from both σ versus pH plots (Fig. 4) and ΔH_{H^+} versus pH plots (Fig. 6), that there are real differences in the acid and base titrations, Hysteresis between acid and base titration

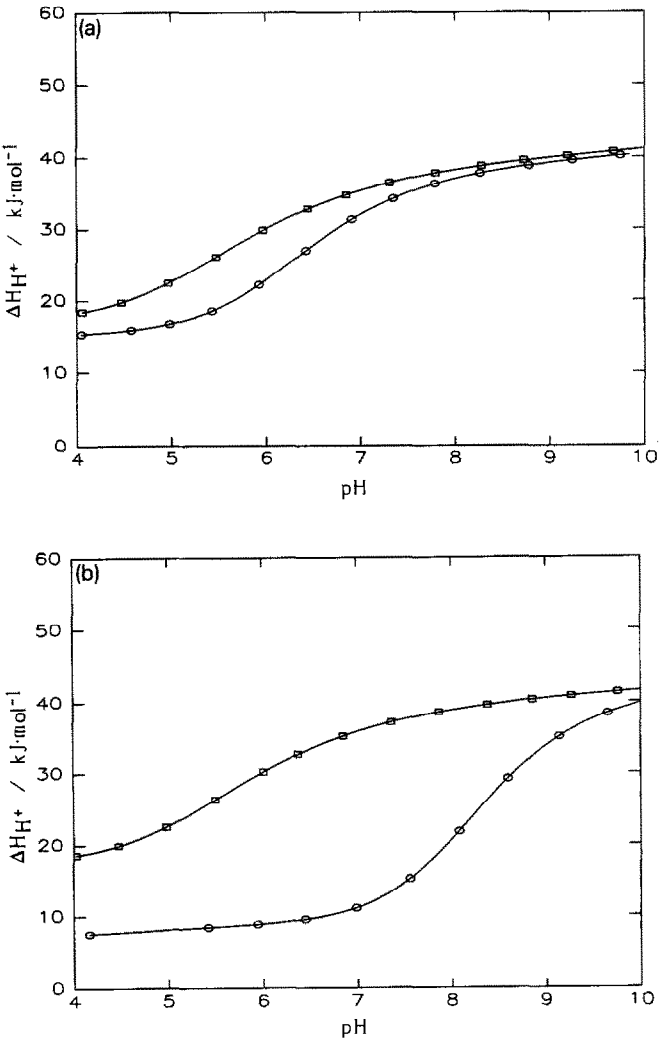

Fig. 6. ΔH_{H^+} in kJ mol^{-1} plotted versus pH for proton ionization from TiO_2 in 0.01 M (Fig. 6a), 0.1 M (Fig. 6b), and 0.5 M (Fig. 6c) NaCl. The curves shown are fits of the titration data using eqn. (12) and the fitting parameters given in Table 1. The lines designated with □ are from the base titration data and lines designated with ○ are from the acid titration data. Increasing the ionic strength from 0.01 M (6a) to 0.1 M (6b) increases the hysteresis, i.e. the difference in the ΔH_{H^+} value calculated at a given pH from the acid and base titration curves.

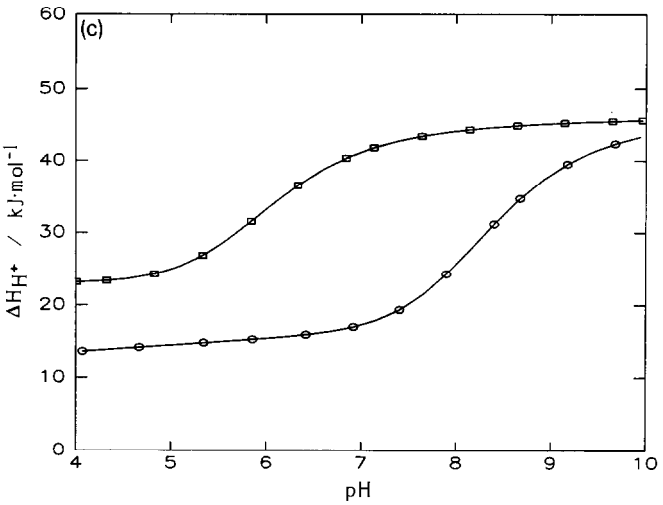

Fig. 6 (continued).

curves has been reported in previous studies but has not been systematically studied or explained. In fact, in a recent calorimetric study of TiO_2, Machesky and Anderson [20] employed the traditional approach of averaging acid and base titration data to "cancel out extraneous reactions."

TABLE 1

A list of the fitting parameters from eqn. (12) for fitting both the acid and base titration data of TiO_2 (10 g l^{-1}) in 0.01, 0.1, and 0.5 M NaCl

[NaCl]	A [a]	B [b]	C [c]	D [d]	E [e]	Standard deviation [f]
Base titrations						
0.01	39.0	20.0	45	5.85	0.7	2.88
0.1	40.5	21.5	45	5.95	0.5	3.49
0.5	45.0	21.5	70	6.1	0.2	2.26
Acid titrations						
0.01	38.5	21.5	70	6.5	0.7	7.31
0.1	41.0	30.5	125	8.25	0.7	4.01
0.5	43.5	26.0	140	8.35	0.9	2.86

[a] A is probably related to ΔH_2 with units of kJ mol^{-1}. The average of ΔH_2 calculated from all of the acid and base data is 41.3 ± 2.5 kJ mol^{-1}.

[b] B is probably related to $(\Delta H_2 - \Delta H_1)$ with units of kJ mol^{-1}. The average of ΔH_1 calculated from all of the base data and the 0.01 M NaCl acid data is 19.6 ± 2.8 kJ mol^{-1}.

[c] C is unitless and not clearly related to any single thermodynamic parameter.

[d] D is probably related to pH^0 the apparent pH at which the surface has a net charge of zero (PZC).

[e] E is probably related to the average electrostatic dependance of ΔH_{H^+}, i.e. $\partial \Delta H / \partial pH$ at the pH extremes.

[f] F is the standard deviation of the fit, with units of kJ mol^{-1}.

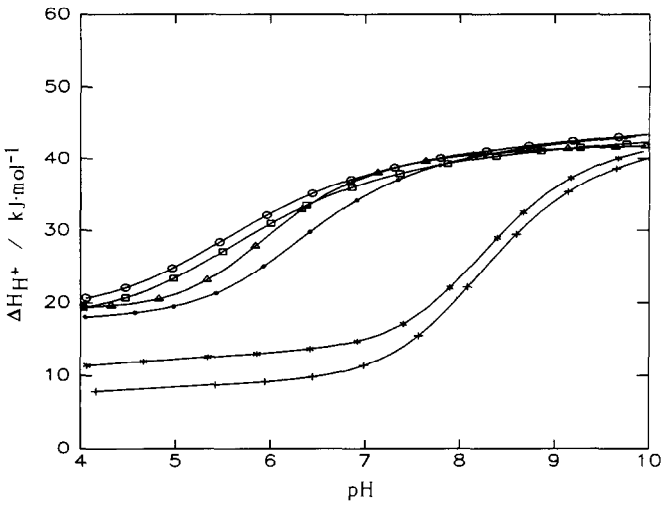

Fig. 7. ΔH_{H^+} in kJ mol^{-1} plotted versus pH for proton ionization from TiO_2 calculated from acid titrations in 0.01 M (●), 0.1 M (+), 0.5 M (★) NaCl and calculated from base titrations in 0.01 M (○), 0.1 M (□), and 0.5 M (△) NaCl. The curves shown are fits of the titration data using eqn. (12). The fitting parameters given in Table 1 have been used, with the exception that average values were used for ΔH_1 and ΔH_2. This was done in order to compare the curves at their respective $pH^{\ominus}$ values and to more clearly demonstrate the trends in ΔH_{H^+} with both ionic strength and titration direction.

In order to study the hysteresis phenomenon, experiments were performed in which titrant was added to the calorimeter at several different rates. In the experiments with the slowest rate of titrant addition, a small aliquot (approx. 0.17 ml) of the acid or base was injected every 30 min until the incremental titration was complete (approx. 3.5 h were required to cover the pH range 4–10). In experiments with a faster rate of titrant addition, the acid or base was added continuously over a time period of either 10 or 40 min (covering the pH range 4–10). The hysteresis, as judged by the difference in the ΔH_{H^+} values in the acid and base titrations near the value of D from eqn. (12), was significantly reduced as the rate of titrant addition was slowed. The approximate rate constant for the slow reaction(s) responsible for the hysteresis is 1 h^{-1}. Differences in the hysteresis observed in TiO_2 titrations in NaCl and in other supporting electrolytes suggest that the slow reaction causing the hysteresis is counterion binding [28].

In order to more clearly determine the effect of ionic strength on ΔH_{H^+}, the acid and base curves from Fig. 6 have been replotted in Fig. 7 after adjusting all of the curves to have the same average value for ΔH_2 (parameter A from eqn. (12)). The largest adjustment made in order to superimpose all of the curves was 3.7 kJ mol^{-1}. As shown in Fig. 7, the base titration curves are largely unaffected by ionic strength changes. This finding is in agreement with results previously published for rutile by Machesky and

Anderson [20]. However, our base titration data do show a small regular increase in pH^0 (parameter D from eqn. (12)) as the ionic strength is increased from 0.01 to 0.5 M. The acid titration data show a much larger ionic strength effect. In the acid titrations the TiO_2 surface appears to be positively charged at pH's as much as 2 pH units above the accepted PZC (note the change in D with electrolyte concentration in Table 1) and ΔH_{H^+} at low pH is much more depressed than in the base titrations, i.e. an indication of higher surface charge due to the slow release of bound cations.

The enthalpy change for proton ionization from TiO_2 is endothermic throughout the pH region 4–10; however the enthalpy change becomes progressively more endothermic as the pH changes from 4 to 10. The titration curve can be divided into three regions. In the first and third regions, well separated from pH^0, the ΔH_{H^+} value changes linearly with pH. The slope at the pH extremes represents the overall electrostatic contribution to the enthalpy change. Extrapolating the ΔH_{H^+} data for all of the curves given in Fig. 7 to their respective pH^0 values, gives the same values for ΔH_1 and ΔH_2, 20.2 and 41.3 kJ mol^{-1} respectively. (The low pH data for 0.1 and 0.5 M acid titrations were not at equilibrium and thus not used in calculating ΔH_1.) In the second region, near pH^0, the ΔH_{H^+} value varies continuously between these intrinsic values. There should also be limiting values for ΔG_{H^+} in regions 1 and 3, with ΔG_{H^+} varying continuously, like ΔH_{H^+}, as the pH goes through pH^0.

The calorimetric data can be used to determine the relative importance of the electrostatic and chemical contributions to the free energy and enthalpy changes. As an initial attempt to model the thermodynamics of ionic interactions at the TiO_2 surface, the free energy and enthalpy changes can be broken down into the following components

$$\Delta G_{H^+} = \Delta G + \Delta G_E \tag{13}$$

$$\Delta H_{H^+} = \Delta H + \Delta H_E \tag{14}$$

where ΔG and ΔH are the intrinsic changes for either the first or second proton ionization, i.e. it is evident from eqns. (1) and (2) that proton ionization should be similar to a diprotic acid, and ΔG_E and ΔH_E are the changes due to electrostatic interactions. The electrostatic interactions can be separated into proton interactions with the charged surface and the influence due to counterion binding. The electrostatic influence on the thermodynamics of an ion binding to a charged surface can be described by eqns. (15)–(17) [29]

$$\Delta G_E = \frac{FeZ_S}{rD} \tag{15}$$

$$\Delta H_E = \frac{FeZ_S}{rD}\left(1 + T\left(\frac{\partial \ln D}{\partial T}\right)_p\right) \tag{16}$$

$$\Delta S_E = \frac{FeZ_S}{rD}\left(\frac{\partial \ln D}{\partial T}\right)_p \tag{17}$$

Where e is the charge on an electron, Z_S is the total surface charge, r is the distance between the counterion and the charged surface, F is again Faraday's constant, and D the solution dielectric constant.

At pH values below the pH of the PZC, the surface of TiO_2 is positively charged. The presence of positively charged neighbor surface sites (i.e. a charged field) repels a proton from the surface, and the ΔG for proton dissociation is more exergonic than ΔG_1, the intrinsic free energy change for the first proton ionization. At high pH a proton is attracted by the negative charges of neighboring sites and is more difficult to ionize. The free energy change will be less exergonic for the surface at high pH than for ΔG_2, the intrinsic free energy change for the second proton ionization. As the pH of the suspension moves further away from the PZC there are more charged sites. Thus the electrostatic contribution to the thermodynamics for proton ionization from a positively or negatively charged surface can be determined from the slopes of the data above and below the PZC, e.g. $\partial \Delta G/\partial$pH or $\partial \Delta H/\partial$pH. There are no charged sites, and therefore no electrostatic influences, at the PZC so ΔG_1 and ΔG_2 as well as ΔH_1 and ΔH_2 can be determined at that pH.

Addition of an electrolyte affects the free energy change for proton ionization. Below the PZC, anions of the electrolyte ion pair with the surface, and the free energy change for proton ionization becomes less exergonic because the proton feels less repulsion from neighboring sites. Above the PZC, cations bind to the surface, and ΔG for proton ionization is more exergonic. Accordingly, the electrostatic influence on proton ionization is reduced (however, the electrostatic influence due to counterion binding will still affect the slope of the data). The effect of adding an electrolyte that binds to the surface will be to reduce the effect of charged neighbor surface sites on proton ionization.

The goal of this study was to develop a technique so that data of sufficient quality could be obtained to begin modeling the thermodynamics of surface reactions. This goal has been met even though some compromises had to be made, e.g. with a slower titration the reproducibility increased at low and high pH, but during longer experiments normal heat losses become significant and are more difficult to correct for.

In summary, thermodynamic information is essential for a complete understanding of proton ionization from mineral oxides. The enthalpy change for reactions at the surface of a colloid can be measured calorimetrically. However, several modifications to a commercial calorimeter are needed to make these measurements. Future work will include comparisons of different ions and their effect on proton ionization from TiO_2 and other mineral oxides.

REFERENCES

1 G.A. Parks and P.L. de Bruyn, J. Phys. Chem., 66 (1962) 967.
2 R.J. Atkinson, A.M. Posner and J.P. Quirk, J. Phys. Chem., 71 (1967) 550.
3 A. Breuwsma and J. Lyklema, Discuss. Faraday Soc., 52 (1971) 324.
4 A. Breuwsma and J. Lyklema, J. Colloid Interface Sci., 43 (1973) 437.
5 R.P. Abendroth, J. Colloid Sci., 34 (1970) 591.
6 H.C. Li and P.L. de Bruyn, Surface Sci., 5 (1966) 203.
7 T.F. Tadros and J. Lyklema, J. Electroanal. Chem., 17 (1968) 267.
8 Y.G. Berube and P.L. de Bruyn, J. Colloid Interface Sci., 27 (1968) 305.
9 Y.G. Berube and P.L. de Bruyn, J. Colloid Interface Sci., 28 (1969) 92.
10 S.M. Ahmed and D. Maksimov, J. Colloid Interface Sci., 29 (1969) 97.
11 L. Blok and P.L. de Bruyn, Colloid Interface Sci., 32 (1970) 518.
12 C.P. Huang and W. Stumm, J. Colloid Interface Sci., 43 (1973) 409.
13 R. Sprycha, J. Colloid Interface Sci., 102 (1984) 173.
14 R. Sprycha, J. Colloid Interface Sci., 110 (1986) 278.
15 P.P. Wu, J. Colloid Interface Sci., 110 (1986) 601.
16 K.F. Hayes, A.L. Roe, G.E. Brown, Jr., K.O. Hodgson, J.O. Leckie and G.A. Parks, Science, 238 (1987) 783.
17 J. Westall and H. Hohl, Adv. Colloid Interface Sci., 12 (1980) 265.
18 P.H. Tewari and A.B. Campbell, J. Colloid Interface Sci., 55 (1976) 531.
19 M.A. Blesa, N.M. Figliolia, A.J.G. Maroto and A.E. Regazzoni, J. Colloid Interface Sci., 101 (1984) 410.
20 M.L. Machesky and M.A. Anderson, Langmuir, 2 (1986) 582.
21 K.A. Wierer and B. Dobias, J. Colloid Interface Sci., 122 (1988) 171.
22 L.G.J. Fokkink, Ion Adsorption on Oxides, Ph.D. disertation, Soil Science, Landbouw University, Wageningen, The Netherlands, May 22, 1987.
23 L.D. Hansen, E.A. Lewise and D.J. Eatough in J.K. Grime (Ed.), Analytical Solution Calorimetry, Wiley, New York, 1985, Chap. 3.
24 D.P. Breziinski, Talanta, 30 (1983) 347.
25 J.A. Davis, R.O. James and J.O. Leckie, J. Colloid Interface Sci., 63 (1978) 480.
26 M.J.G. Janssen and H.N. Stein, J. Colloid Interface Sci., 109 (1986) 508.
27 J.A. Davis and A. Cook, unpublished data.
28 S.R. Mehr, D.J. Eatough, L.D. Hansen, E.A. Lewis, and J.A. Davis, J. Colloid Interface Sci., submitted for publication 1989.
29 E.A. Lewis, J. Barkley and T. St. Pierre, Macromolecules, 14 (1980) 546.